SCIENTIFIC PAPER
Published: October 26, 2023
https://doi.org/10.13167/2023.27.7

Magnetic pole repulsive damper (MPRD): A promising solution for seismic protection of structures

Hemnath Kasaram[1], Amudhan Vijayakumar[1], Daniel Cruze[1] and Saran Sathish Kumar[1]

[1] Hindustan Institute of Technology and Science, Department of Civil Engineering, Chennai, Tamil Nadu, India

Corresponding author:
Daniel Cruze
danielckarunya@gmail.com

Received:
May 18, 2023

Accepted:
July 24, 2023

Published:
October 26, 2023

Citation:
Kasaram, H.; Vijayakumar, A.; Cruze, D.; and Kumar, S. S. (2023). Magnetic pole repulsive damper (MPRD): A promising solution for seismic protection of structures. *Advances in Civil and Architectural Engineering*. Vol. 14, Issue No. 27. pp. 97-113
https://doi.org/10.13167/2023.27.7

ADVANCES IN CIVIL AND ARCHITECTURAL ENGINEERING (ISSN 2975-3848)

Faculty of Civil Engineering and Architecture Osijek
Josip Juraj Strossmayer University of Osijek
Vladimira Preloga 3
31000 Osijek
CROATIA

Abstract:
Owing to its high energy dissipation characteristics, the passive damper is an effective means of mitigating natural hazards for structures. In this study, a novel magnetic pole repulsive damper (MPRD), designed for reducing structural responses during natural hazards such as earthquakes, was developed and its performance was validated. The MPRD is an effective solution for seismic protection that works on the principle of magnetic repulsion and has a higher energy dissipation capacity than conventional dampers. The MPRD was fabricated using mild steel, neodymium magnets, and a set of helical springs. Two scaled reinforced concrete frames were tested using a 50 kN loading actuator. One frame was equipped with the MPRD, while the other served as a conventional frame for comparison. The frame with the MPRD showed reduced displacements. Compared with the conventional frame, that with the MPRD exhibited an increase in load of 40 % and an increase in energy dissipation of 6,44 %. Further, an increase in lateral stiffness, a 19,23 % increase in stiffness degradation, and changes in crack patterns were observed in the frame with MPRD compared to the conventional frame. The study's success in validating the MPRD performance in reducing structural responses in moderate to high seismicity regions makes it a promising solution for building seismic protection.

Keywords:
magnetic pole repulsion damper (MPRD); RC frame; cyclic loading; energy dissipation; lateral stiffness

1 Introduction

In recent decades, numerous catastrophic earthquakes have occurred, such as the recent events in Turkey and Syria. The rising number of casualties resulting from building collapse and structural damage highlights the severe seismic risks involved. To mitigate these hazards, it is imperative to design or retrofit residential, lifeline, historical, and industrial structures meticulously to ensure their protection against earthquakes [1]. Earthquakes cause billions of dollars in damage and hundreds of deaths annually. It is increasingly important for engineers to design buildings that can withstand seismic forces. Engineers have been working hard to create and develop technologies that can avoid or reduce the effects of seismic events, such as earthquakes. Dampers are a type of seismic vibration control device; other varieties include active, semi-active, and hybrid devices (combinations of the previous three) [2-6].

Older reinforced concrete (RC) buildings with insufficient lateral force-resistant systems are prone to substantial damage during seismic events [7-9]. However, such facilities continue to exist in nations that have only recently acknowledged seismic hazards and possess limited seismic design practices. Regrettably, this issue commonly impacts public establishments such as educational institutions and healthcare facilities, which offer shelter and medical assistance in times of calamity. Contemporary seismic design codes assign higher design requirements to public structures to mitigate damage and facilitate immediate occupancy. Nevertheless, RC structures constructed before the implementation of seismic loads or using an outdated seismic design code require appropriate retrofitting measures. However, a different course of action is required to strengthen this plan. Energy dissipation dampers are among the most frequently used practical techniques for enhancing the seismic performance of structures [10]. In addition, the retrofitting process may include the installation of new reinforced concrete (RC) shear walls to fill the bays [11] or the incorporation of traditional steel braces [12]. The performance of dampers has been demonstrated to enhance the seismic performance of newly constructed buildings and effectively regulate the seismic response of retrofitted buildings, resulting in energy dissipation. This finding is supported by previous studies [13, 14]. In recent decades, many energy-dissipation technologies (such as friction dampers, viscoelastic dampers, and fluid dampers) have been developed in addition to the aforementioned structural strengthening techniques to enhance the seismic performance of structures. Among these energy-dissipating devices, metallic dampers have drawn increasing attention and emerged as the preferred dampening option for seismic retrofitting [15]. Passive magnetic dampers are an option because they are designed and manufactured to react to vibrations in a certain manner without the need for active feedback and control. They are flexible and adjustable during the construction process. Kim developed an adjustable friction damper that uses steel wires and permanent magnet cubes to dissipate energy, and pre-compressed polyurethane springs to provide a re-entering force. The initial testing showed that applying a damper to a braced-frame structure could improve its seismic performance by preventing permanent deformation. Further studies are being conducted on this damper. A diagonal semi-active damper was used to investigate the seismic response of a reduced one-storey RC frame. The damper was tested with electrical currents of 0 and 3 A, producing a dampening force of 5,83 kN. A multiple-coil magnetorheological damper was used to perform a time-history analysis [16]. In Sinha's [17, 18] investigation, fluid viscous dampers (FVDs) were studied and found to be widely used because of their effectiveness in reducing the stress demands on structural elements and shear forces. FVDs achieve this by reducing the damping demands on structural members through frictional and hysteretic damping of the damper brace system. This results in lower hysteretic damping by the structural members and less inelastic behaviour, which prevents damage to the structural members. FVDs are displacement-based devices that focus more on response control than on energy dissipation. Javidan [19] studied a steel column damper on two RC frames to assess its seismic efficacy. The damper dissipated energy through a steel column and two fused sections. The study validated the analytical model through experiments and found that retrofitting with a damper effectively mitigated inter-storey drift and reduced structural damage, demonstrating that dampers can improve seismic

performance. Dilsiza [20] studied the seismic behaviour of a 15-storey RC special moment-resistant frame (RC SMRF) in Turkey.

In this study, an RC SMRF system with viscous wall dampers (VWDs) was compared to a conventional SMRF system without damping devices. This study found that installing VWDs can improve the seismic performance of RC SMRF structures, and is a feasible retrofitting approach. Installing VWDs on the lower levels of a building effectively decreases the floor acceleration values and improves the inter-storey shear pressures and base shear. Hur [21] studied the mechanical characteristics of the Kagome truss damper and proposed a wall-type Kagome damping system (WKDS) for the seismic retrofitting of existing RC structures. The WKDS was evaluated through tests and analysis and showed increased stiffness, strength, energy dissipation, and seismic damage mitigation in RC frame structures. This study recommends using the WKDS for retrofitting existing structures to improve their seismic resilience. This approach uses friction dampers for performance-based applications, and it has recently attracted significant interest among researchers. Balendra [22] investigated the use of multilevel control systems that incorporate friction dampers to effectively dissipate energy during earthquakes of varying intensities. Bagheri [23] focused on implementing U-shaped metallic yielding dampers with rotating friction dampers in steel building frames. Aghlara [24] introduced a bar-fuse damper (BFD) and studied its application to enhance the seismic performance of precast concrete (PC) frame structures. Wu [25] proposed the use of sector-lead viscoelastic dampers (SLVDs) to repair damaged RC frames. Zhang [26] investigated the use of sector-lead viscoelastic dampers (SLVDs) to improve the seismic performance of RC frames. Bruschi [27] introduced a novel friction damper, the prestressed lead damper (PS-LED), which effectively dissipates seismic energy through controlled friction between a steel shaft and a prestressed lead core. Experimental characterisation and numerical modelling demonstrated stable behaviour, a high damping ratio, and accurate predictions. The PS-LED proved beneficial in reducing lateral deformation and controlling structural accelerations and internal forces. Future research should include testing prototypes with varying dimensions, exploring the relationship between prestress and strength for design optimisation, and investigating the performance of buildings with PS-LEDs under different seismic scenarios. In the study of Fathizadeh [28, 29], nonlinear analyses focused on improving the seismic performance of multi-storey curved damper semi-rigid moment frames (CDSRMFs). The addition of curved dampers enhanced stiffness, strength, and energy dissipation. Plastic hinges are mainly formed in-curved damper elements rather than in primary structural elements, making them easily replaceable. The CDSRMFs are reliable and resilient to seismic forces. Further research is recommended to optimise damper dimensions using algorithms for better seismic performance and also to develop a cost-effective curved damper truss moment frame (CDTMF) system that combines curved dampers and steel trusses for seismic energy dissipation. Optimised CDTMF prototypes surpass the buckling restrained knee braced truss moment frame (BRKBTMF) systems in various performance aspects, meeting the FEMA P695 requirements and facilitating the easy replacement of components damaged during earthquakes. Aydin [30] focused on improving the stability and seismic performance of structures by optimising viscous dampers. They explored three methods utilising transfer functions to optimise dampers by considering displacements, accelerations, and shear forces. Aydin demonstrated that strategically placing dampers based on transfer function analysis leads to better outcomes, reducing displacements, accelerations, and shear forces. This highlights the importance of optimising dampers to enhance seismic performance and improve structural stability during earthquakes. Khalili [31] proposed a novel damper design using hourglass-shaped steel pins to reduce the seismic energy in steel connections. Experimental and numerical tests confirmed its effectiveness in dissipating energy while maintaining connection resistance. Implementing the damper improves the ductility and seismic resilience. It is suitable for steel construction in medium-to-high seismicity regions and offers cost savings. Further research is needed to validate its applicability to different structures and to conduct shaking table tests to obtain more reliable results.

A magnetic pole repulsive damper (MPRD), which is a unique passive damper that uses magnetism and spring characteristics to oppose seismic waves on structures, was developed in this study. Without additional power or control systems, the MPRD functions based on magnetic repulsion. Using the repulsive force between the magnetic poles and the spring, it dissipates energy and withstands seismic wave-induced motion. It provides damping under various seismic circumstances and reacts to them, improving structural stability and building safety. The MPRD can withstand seismic waves without the need for active control mechanisms or outside power.

2 Methodology

2.1 Damping system

Passive dampers reduce vibrations or oscillations in a system without requiring external power or control [32]. They include tuned mass dampers, base isolation systems, and energy-dissipating devices implemented in structural engineering to mitigate seismic forces [33]. Passive dampers function autonomously, are cost-effective, have low maintenance requirements, and do not require feedback. These dampers mitigate the inelastic energy dissipation in a structure's framing system, resulting in reduced structural damage, cost savings, and preservation of life and the environment.

2.1.1 Magnetic pole repulsive damper

The proposed MPRD is a passive damping device made of stainless steel that utilises magnetic repulsion to reduce building seismic vibrations. It consists of neodymium magnets, detachable plates, pistons, and springs. The damping system of the device balances the directional flow of seismic activity through compression and tension. The lower spring undergoes compression owing to magnetic repulsion. By contrast, the spring over the piston rod has tension and compression, and the magnet has damping characteristics, making it a hybrid passive damper. The device, made of durable and hygienic stainless steel, is cost-effective. Figure 1 depicts a detailed schematic description of the proposed MPRD.

2.1.2 Experimental results of spring and magnet

The experimental results indicated that the spring experienced a compression force of 2,196 kN and tension force of −1,972 kN at a maximum displacement of 25 mm. The neodymium magnet exhibited a maximum repulsive force of 1,3894 kN at a displacement of 5 mm, which decreased to 0,7 kN at a 25 mm displacement. These results suggest that the spring was compressed and stretched by the respective forces, whereas the repulsive force on the magnet decreased with increasing distance [34-36].

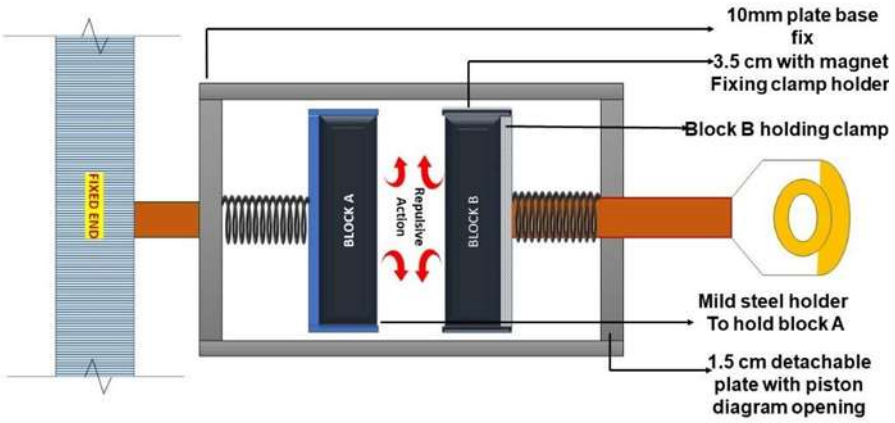

Figure 1. Schematic representation of magnetic pole repulsive damper (MPRD)

2.2 Moment-resisting frame

2.2.1 Positioning of the damper in frames

Dampers are frequently used in structural engineering to reduce the impact of seismic forces on buildings, and the orientation of dampers within a frame structure is an essential consideration in their design. The different damper orientations include diagonal, cross, chevron, and K-shaped configurations, which were studied to evaluate their effectiveness and ease of installation. Each orientation has advantages and disadvantages in mitigating seismic forces, and these studies have helped engineers optimise damper design and placement for improved seismic resilience. Owing to their cost-effectiveness and high dissipative capacity, these frames are extensively utilised in single- and multi-storey buildings [37-39].

2.2.2 Scaling and detailing of the reinforced concrete frame

Owing to the limitations of the experimental setup, the configuration of the two-storey RC building was scaled down to 1:3. Two specimens were tested thoroughly according to a specific protocol [40]. Specimen S_1 represented the conventional bare frame, whereas specimen S2 featured an MPRD integrated into the frame. The study primarily focused on a regular frame consisting of a footing (1,60×0,56×0,10 m), two columns (1×0,077×0,077 m), and a beam (1× 0,077×0.077 m) with high-strength wire shear reinforcements. The design of the frame was based solely on gravity loads, following the provisions outlined in IS 456:2000 [27, 41]. Stirrups with 90° end hooks were used for each member, and the columns were subjected to essential shear fortification. The RC footing was intentionally strengthened to ensure that it possessed sufficient strength to withstand the test without sustaining any damage. Figure 2 shows the dimensions and reinforcement details of the tested RC frame.

2.3 Study of materials

Most RC frames consist of concrete and reinforced steel. However, variations in quality control during construction can lead to deviations from the intended design values. Therefore, it is essential to accurately determine the material properties to ensure compliance with RC building regulations. The fundamental characteristics of steel and concrete play a crucial role in understanding the behaviour of bare frames under different stress conditions. According to Indian standards (IS 1786:2008) [42], the Fe415 steel used in this study's design mix for M25 concrete has a tensile strength of 485 MPa. Grade 53 cement was used in this study. Thermomechanical treated bars (TMT) bars served as the primary reinforcement for the frame members. These bars have a yield strength of 415 MPa, and high-tension cables were used for shear reinforcement instead of conventional reinforcements in beams and columns.

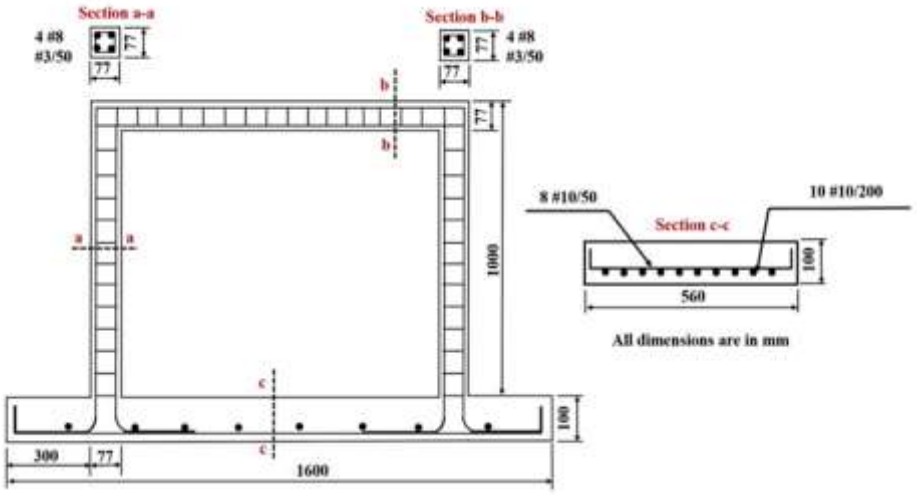

Figure 2. Details of reinforcement in the scaled-bare frame

2.3.1 Concrete mix design

An RC structure was constructed using locally available natural sand, coarse aggregates, steel, and ordinary Portland cement (grade 53). The physical properties of the cement (Table 1), sand, and aggregates were evaluated according to the IS 10262:2019, the Indian standard code for mix design of M25 grade concrete 1:1,60:2,47. The characteristics of the fine and coarse aggregates are listed in Table 2, and Figure 3 shows a sieve analysis graph of the fine and coarse aggregates. The sieve analysis results indicated that the fine and coarse aggregates met the requirements specified in the IS 10262:2019 code for a target compressive strength of 25 MPa.

Concrete cubes with dimensions of 150×150×150 mm were prepared for the compression tests, as illustrated in figure 4. According to the instructions provided in IS 10262:2019, the cubes were cast using the mix design of M25 for testing on days 7, 14, and 28. A universal testing machine with a capacity of 200 T was used. The average compressive strength of the concrete after 28 d was determined to be 30,1 MPa. However, on the day of testing, it was found to be 31,7 MPa, which indicated a slightly higher strength. The compressive test results are presented in Table 3.

Table 1. Physical characteristics of the cement

Physical properties	Observed values	Desired values
Target coherence	28,50 %	Nil
Commencing phase	110 min	> 30 min
Ultimate phase	320 min	< 600 min

Table 2. Physical characteristics of the fine aggregate and coarse aggregate

Property	Coarse aggregate	Fine aggregate
Specific gravity	2,70	2,65
Water absorption (%)	0,34	1,12
Bulk density (kg/m^3)	1485	1620

Table 3. Compressive strength of cubes

Physical properties	Observed values (MPa)	Desired values (MPa)
7 days	18,25	17
14 days	24,10	23
28 days	31,70	29

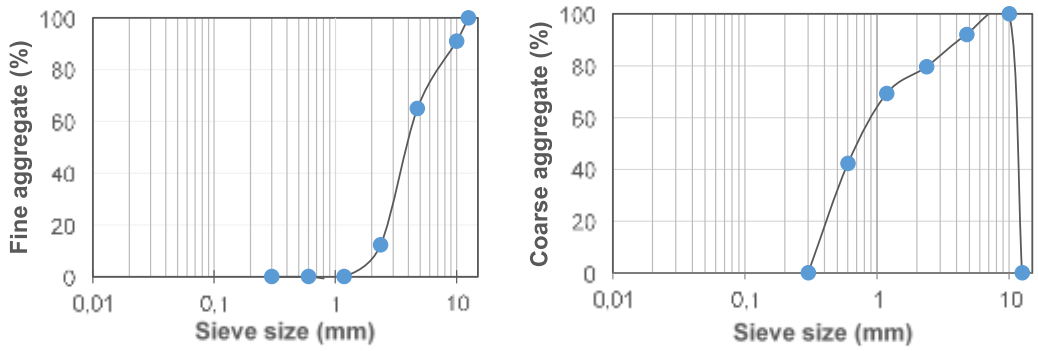

Figure 3. Sieve analysis of fine and coarse aggregates

Figure 4. Casting of cubes and testing in the universal testing machine

3 Casting of reinforced concrete frame

The moment-resisting frames were built using vertically cast components to simplify the pouring of concrete. The mould for the frame was built using plywood with an allowance of 3 mm. The plywood was oiled, as shown in Figure 5, to easily remove the specimen from the mould after the casting was performed. The centring work for the specimen was carried out according to the reinforcing details shown in Figure 2. The centrifugation process is shown in Figure 6a. The specimens were cast using a wooden mould and M25-grade concrete. Figure 6b illustrates the casting of the RC frame. The base was reinforced and kept in a mould for concrete pouring. The casting process started at the base of the frame and continued to the beam and column of the frame. Figure 6b shows the completed framework after tampering with a rod to finish the levelled frame evenly. All specimen members were compressed manually, and the frame parts were effectively cured by covering them with gunny bags and spraying them with water regularly.

Figure 5. Plywood formwork painted with oil

(a) (b)

Figure 6. a) Centring work and b) casting of the reinforced concrete (RC) frames

3.1 Test specimens

A single-span frame configuration was adopted for the experiment, and a miniaturised moment resisting frame (MRF) was used. Two different configurations were cast: a bare frame without additional features (S_1) and a frame incorporating an MPRD for enhanced performance (S_2). Specific details of the two test specimens are presented in Figure 7.

3.2 Experimental detail of frames with proposed MPRD and base fixtures

The cyclic loading test involved displacement control, and was conducted using an MTS machine equipped with an actuator that could expand and contract, allowing for a maximum displacement of 0,125 m in both directions. The experimental setup and loading patterns are shown in Figures 9 and 10, respectively. The loading frame has a maximum capacity of 250 kN and is equipped with transducers to measure the load and movement within the frame.
The actuator was positioned 1100 mm above the base platform and fastened with nuts and bolts via ten holes with a 30 mm diameter to provide stability and reduce frame movement during testing. This setup provided rigidity to the system. Additionally, wooden blocks were securely fastened at both ends of the footing to minimise the longitudinal movement and serve as frictional brakes, effectively preventing sliding.

3.3 Experimental test setup

The load cell and linear variable differential transformer (LVDT) are the two critical components in the cyclic loading test. The load cell and transducer were linked to the actuator, allowing lateral strength and displacement to be measured on the west side. On the east side, one LVDT monitored the displacement of the beam horizontally, whereas two LVDTs at the top and bottom detected the movement on both sides. The LVDT needle spanned 0,055 m and allowed the piston to travel 50 mm in all directions. The LVDTs were set in place on both frames, with and without the MPRD. The data-gathering technology used was sophisticated, allowing the collection of findings with precision and accuracy, as shown in Figures 7 and 8.

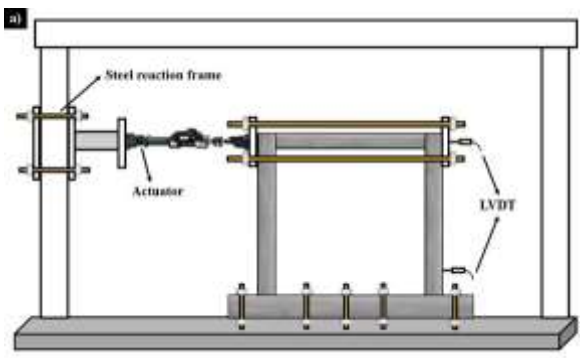

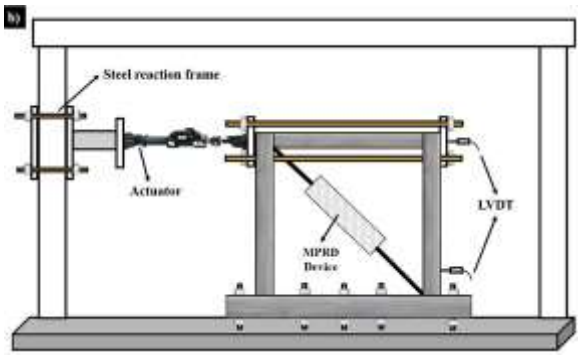

Figure 7. Experimental setup: (a) bare frame and (b) frame with MPRD

Figure 8. RC frame subjected to cyclic loading with MPRD

3.4 Loading history

The specimens were designed to absorb seismic energy cyclically, and their stiffness, damage propagation, lateral strength, and energy dissipation were tested using static cyclic loading. In the load control mode, cyclic lateral loads were applied to the left-side corners of the specimens. The applied load determined the number of loading cycles that were applied horizontally at a predetermined rate. As indicated by the loading curve, the loading pattern employed in this investigation featured force versus displacement, and each cycle was repeated twice. A displacement interval of 2,5 mm for 0-10 mm displacement and a 5 mm interval for 10-35 mm displacement were used. Figure 9 shows the loading history of the frame.

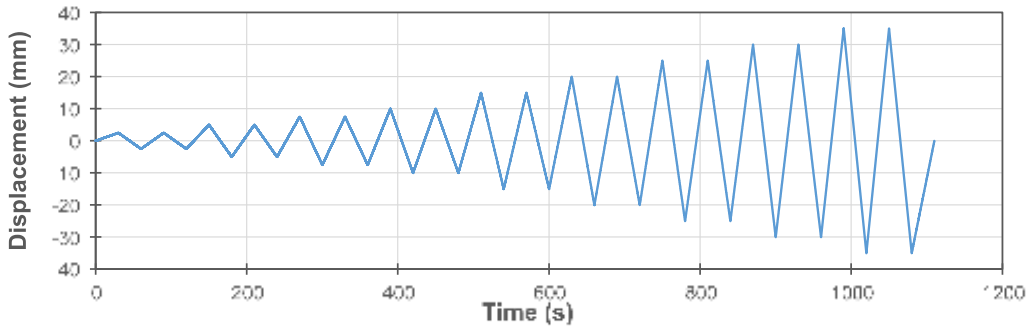

Figure 9. Loading pattern

4 Results and discussion

4.1 Lateral load-carrying capacity

A cyclic test was performed to evaluate the frame capacity with and without the MPRD device. This experiment helped determine the stability of the MPRD device in the frame. The major results are presented in Table 4, including the moment of appearance of the first crack and the ultimate load achieved.

Table 4. Observed lateral load-carrying capacity

Specimen	First shear crack (kN)	First shear crack displacement (mm)	Ultimate load (kN)	Maximum displacement (mm)
Specimen 1 without MPRD	-2,32	-5	5,210	25
Specimen 2 with MPRD	-4,51	-10	9,264	35

4.2 Hysteretic behaviour

A hysteretic loop is a graphical depiction of a material's stress–strain relationship after repeated loading and unloading cycles. It demonstrates the reaction of the material throughout the loading and unloading phases and can provide insights into its behaviour and qualities, such as stiffness, strength, and energy dissipation capabilities. In the test, each cycle was run twice, and the loop formation determines the maximum load at a given displacement. The specimen with no MPRD (the bare frame) measured 5,55 kN in the positive direction and −6,60 kN in the adverse order, as shown in Figure 10. In the MTS cyclic loading test, the specimens with the MPRD had loads of up to 9,26 kN in the positive direction and −8,01 kN in the adverse order, as shown in Figure 11.

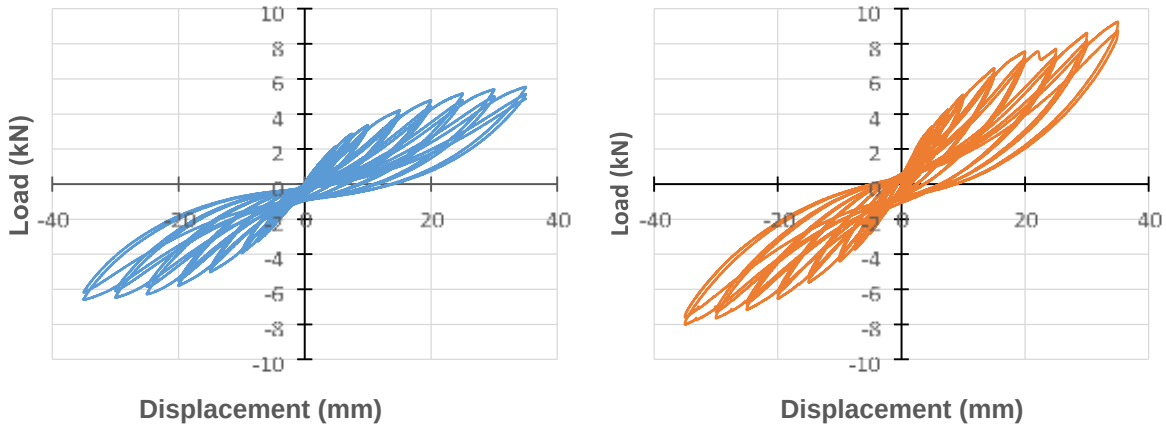

Figure 10. Hysteretic behaviour of the moment resisting frame (MRF) frame without MPRD (blue) and with MPRD (orange)

4.3 Stiffness degradation

The stiffness degradation graph shows a reduction in the strength or stiffness of the frames with and without the MPRD owing to cyclic loading. The secant stiffness of the specimen was obtained using the extreme loads and displacements in both positive and negative directions. As the displacement levels increased, the stiffness decreased continuously owing to the cumulative damage in the specimens, leading to severe stiffness degradation at the end of the tests. The graph shown in Figure 11 is an essential tool for designing earthquake-resistant structures and predicting the long-term behaviour of materials and structures. Comparing the

frames with and without MPRD, the stiffness degradation of the frame with MPRD was 19,23 % higher than that of the bare frame.

$$Ki = (|+Ai| + |- Ai|)/ (|+Di| + |- Di|) \quad (1)$$

Here, Ai and Di represent the peak resistance and applied displacement at cycle i, respectively.

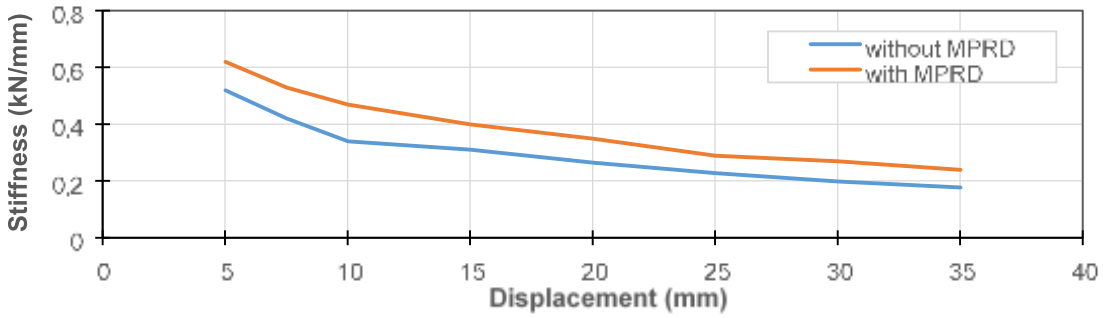

Figure 11. Stiffness degradation of MRF with and without MPRD

4.4 Backbone curve

In structural engineering, the backbone curve is a graphical representation of the relationship between the shear force and bending moment at critical locations in a moment-resisting frame. This helps predict the behaviour of the frame under different loading cycles and design and analyse moment-resisting frames. The term can also refer to the relationship between the applied load and lateral displacement at a specific point, which helps analyse the strength of a moment-resisting frame and its stiffness characteristics, respectively. Figure 12 compares the backbones of the two frames with and without the MPRD. The backbone curve can be used to determine the maximum load at a displacement from the hysteresis loop, and to compare the difference between a frame with an MPRD and a bare frame.

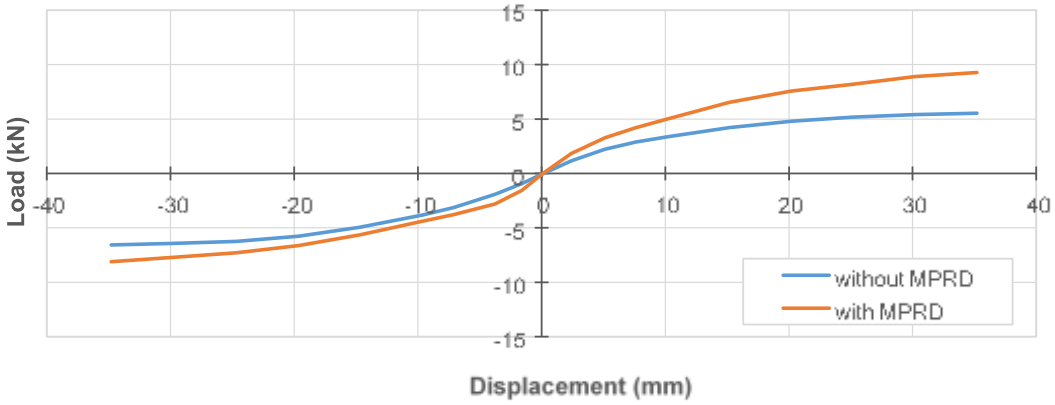

Figure 12. Backbone curve of MRF with and without MPRD

4.5 Lateral stiffness

The lateral stiffness was measured by calculating the line slope between the positive and negative load–displacement cycles. The two specimens were compared at different displacement levels. The frame with MPRD had higher initial lateral stiffness than the bare frame, with a difference of 58,72 % at 2,5 mm displacement (Figure 13). However, the lateral stiffness decreased as the lateral displacement increased in both specimens. Overall, the MPRD increased the lateral stiffness compared with that of the bare frame.

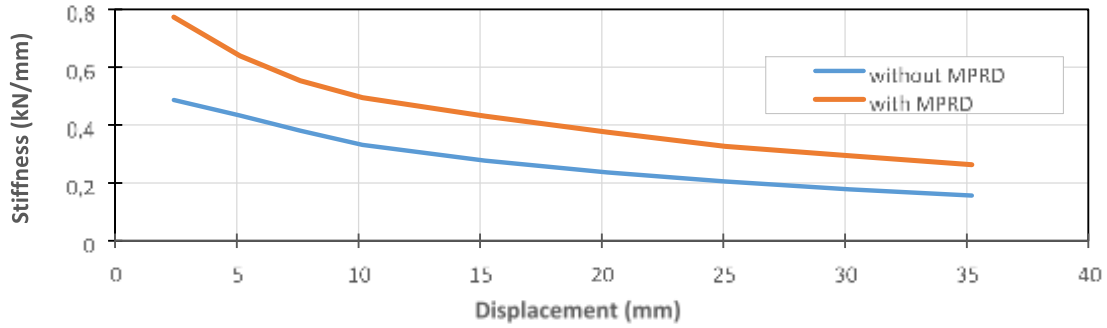

Figure 13. Lateral stiffness of MRF with and without MPRD

4.6 Energy dissipation

MPRD systems can enhance the energy dissipation capacity of a structure. The findings of this study revealed that the frame equipped with the MPRD exhibited significantly higher energy dissipation than the bare frame, as depicted in Figure 14. The MPRD system was designed to dissipate energy and safeguard structures during seismic events. The energy dissipation of the specimens was determined by calculating the area under the hysteresis cycle. S_1 demonstrated an energy dissipation of 213,30 kN.mm at a displacement of 35 mm, whereas S_2 exhibited an energy dissipation of 227,04 kN.mm at the same displacement. Overall, the energy dissipation in S_2, the frame with MPRD, was 6,44 % higher than in S_1 [42].

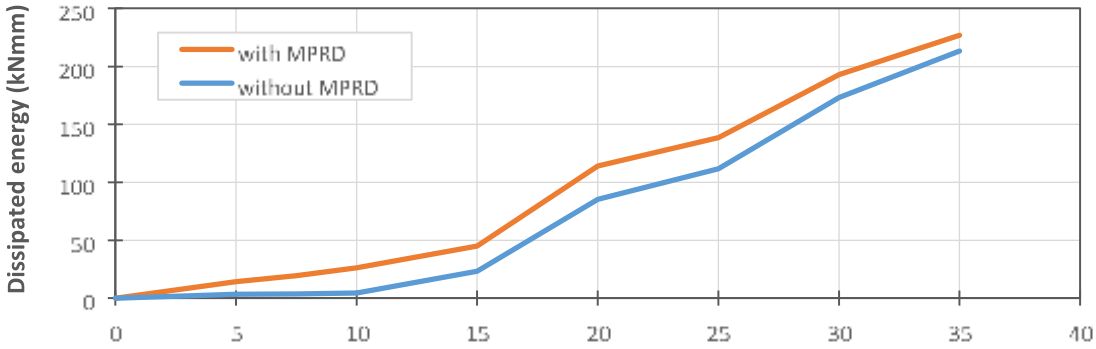

Figure 14. Energy dissipation of MRF with and without MPRD

4.7 Crack patterns

During the cyclic loading test of the RC frame, cracks were observed at specific displacement points. The first crack appeared at −5,0 mm on the structure's foundation in the bare frame, followed by cracks at 7.5 mm and −7,5 mm. Approximately 40 % of the frame failures occurred at −20,0 mm, and the total base failures were observed at +25,0 mm with a crack width of 7,5 mm at the end of the experiment at 35 mm near the joint of the column and base. The crack pattern in the bare frame is shown in Figure 15. In contrast, when the RC frame was equipped with an MPRD device, an initial crack occurred at −10 mm on the left side of the foundation. The second and third cracks appeared at 15 mm and −15 mm, respectively, on the right side of the foundation and top flange, respectively. At a displacement of −30 mm, approximately 80 % of the cracks were observed on the right side of the column near the base, with maximum crack width of 3.0 mm, and a fixed base failure occurred at 35 mm. Notably, the MPRD exhibits substantial magnetic repulsion at a displacement of 25 mm, as depicted in Figure 16.

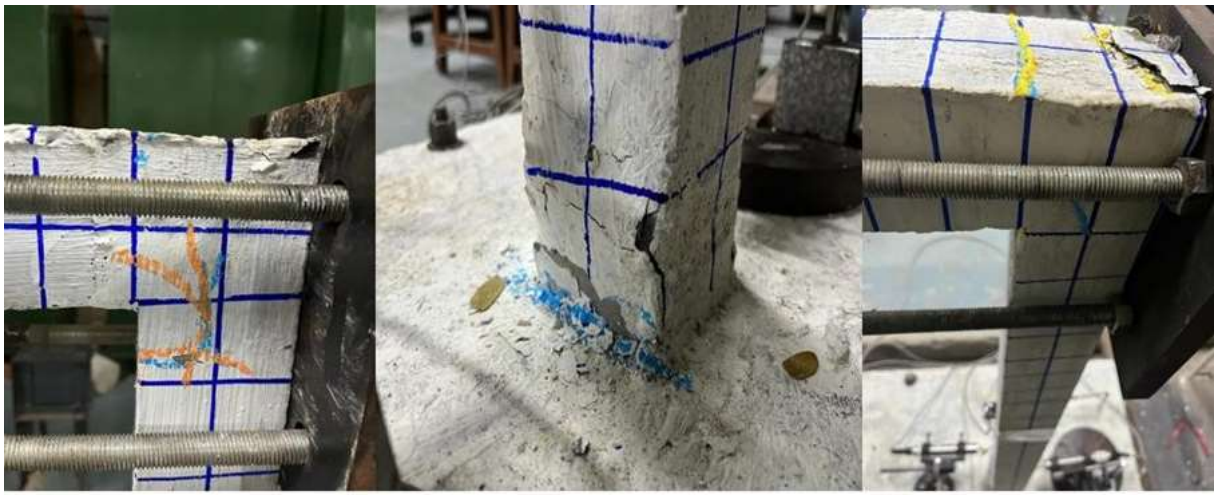

Figure 15. Crack pattern of the RC frame without MPRD

Figure 16. Crack pattern RC frame with MPRD

5 Conclusion

In this study, a passive MPRD system was developed, which, diagonally placed, can increase the earthquake resilience of an RC frame.
The force generated by the frame with MPRD is higher than that produced by the bare frame. The results obtained from the hysteresis curve of the damper satisfy the design requirements.

- The frame equipped with the MPRD system exhibited a significant increase in force, with an overall increment of 38,70 % compared with that of the bare frame.
- A comparative study evaluated the frame with and without the MPRD with respect to various factors, including the hysteretic loop, backbone, crack pattern, energy dissipation, stiffness degradation, and lateral stiffness. The results showed that the frame with the MPRD had better seismic performance than the bare RC frame.
- In to the hysteretic loop graph, the bare frame specimen showed values of 5,55 kN in the positive direction and −6,60 kN in the adverse order. Meanwhile, the specimen with the MPRD reached loads of up to 9,26 kN in the positive direction and −8,01 kN in the negative direction during the MTS cyclic loading test.
- The stiffness degradation of the frame with MPRD was 19,23 % greater than that of the bare frame.
- The frame with MPRD had higher initial lateral stiffness than the bare frame, with a difference of 58,72 % at 2,5 mm displacement.
- The energy dissipation of the frame with MPRD was 6,44 % higher than that of the bare frame.

In future research, the MPRD should be tested with modifications, specifically using the steel moment frame as the testing platform. This will make it possible to evaluate the performance and effectiveness of the damper under different conditions and explore potential enhancements or optimisations.

Abbreviations

BRKBTMF - buckling restrained knee braced truss moment frame
CDSRMFS - curved damper semi-rigid moment frames
CDTMF - curved damper truss moment frame
MPRD - magnetic pole repulsive damper
MRF - moment resisting frame
PS-LED - prestressed-lead damper
S - specimen
S_1 - bare frame
S_2 - frame equipped with an MPRD damper

Acknowledgments

The author expresses their gratitude and acknowledges the support and facilities provided by the Structural Laboratory of the Department of Civil Engineering at Karunya University. The author appreciates the experimental facilities and setup made available to them during their research.

References

[1] Titirla, M. D. A State-of-the-Art Review of Passive Energy Dissipation Systems in Steel Braces. *Buildings*, 2023, 13 (4). https://doi.org/10.3390/buildings13040851
[2] Spencer Jr., B. F.; Nagarajaiah, S. State of the art of structural control. *Journal of Structural Engineering*, 2003, 129 (7), pp. 845-856. https://doi.org/10.1061/(ASCE)0733-9445(2003)129:7(845)

[3] Saaed, T. E.; Nikolakopoulos, G.; Jonasson, J.-E.; Hedlund, H. A state-of-the-art review of structural control systems. *Journal of Vibration and Control*, 2013, 21 (5), pp. 919-937. https://doi.org/10.1177/1077546313478294

[4] Soong, T. T.; Spencer Jr., B. F. Supplemental energy dissipation: state-of-the-art and state-of-the-practice. *Engineering Structures*, 2002, 24 (3), pp. 243-259. https://doi.org/10.1016/S0141-0296(01)00092-X

[5] Symans, M. D. et al. Energy dissipation systems for seismic applications: current practice and recent developments. *Journal of Structural Engineering*, 2008, 134 (1), pp. 3-21. https://doi.org/10.1061/(ASCE)0733-9445(2008)134:1(3)

[6] Tiwary, A.; Tiwari, A.; Kumar, A. State-of-art in active, Semi-Active, and Hybrid Control Systems for Tall Buildings. *International Journal of Engineering Research and Applications (IJERA)*, 2014.

[7] Mitchell, D. et al. Damage to concrete structures due to the 1994 Northridge earthquake. *Canadian Journal of Civil Engineering*, 1995, 22 (2), pp. 361-377. https://doi.org/10.1139/l95-047

[8] Mitchell, D. et al. Damage to concrete structures due to the January 17, 1995, Hyogo-ken Nanbu (Kobe) earthquake. *Canadian Journal of Civil Engineering*, 1996, 23 (3), pp. 757-770. https://doi.org/10.1139/l96-886

[9] Lukkunaprasit, P. et al. Performance of structures in the Mw 6.1 Mae Lao earthquake in Thailand on May 5, 2014, and implications for future construction. *Journal of Earthquake Engineering*, 2016, 20 (2), pp. 219-242. https://doi.org/10.1080/13632469.2015.1051636

[10] Cheraghi, A.; Zahrai, S. M. Innovative multi-level control with concentric pipes along brace to reduce seismic response of steel frames. *Journal of Constructional Steel Research*, 2016, 127, pp. 120-135. https://doi.org/10.1016/j.jcsr.2016.07.024

[11] Canbay, E.; Ugur, E.; Ozcebe, G. Contribution of Reinforced Concrete Infills to Seismic Behaviour of Structural Systems. *ACI Structural Journal*, 2003, 100 (5), pp. 637-643.

[12] Cao, X.-Y. et al. Seismic retrofitting of existing frame buildings through externally attached sub-structures: State of the art review and future perspectives. *Journal of Building Engineering*, 2022, 57. https://doi.org/10.1016/j.jobe.2022.104904

[13] Kim, Y. C.; Lee, H. W.; Hu, J. W. Experimental Performance Evaluation of Elastic Friction Damper. *Case Studies in Construction Materials*, 2023, 18. https://doi.org/10.1016/j.cscm.2023.e01823

[14] Cruze, D. et al. Seismic performance evaluation of a recently developed magnetorheological damper: experimental investigation. *Practice Periodical on Structural Design and Construction*, 2021, 26 (1). https://doi.org/10.1061/(ASCE)SC.1943-5576.0000544

[15] Lee, C.-H.; Ryu, J.; Ju, Y. K. Improving seismic performance of non-ductile reinforced concrete frames through the combined behavior of friction and metallic dampers. *Engineering Structures*, 2018, 172, pp. 304-320. https://doi.org/10.1016/j.engstruct.2018.06.045

[16] Javidan, M. M.; Chun, S.; Kim, J. Experimental study on steel hysteretic column dampers for seismic retrofit of structures. *Steel and Composite Structures*, 2021, 40 (4), pp. 495-509. https://doi.org/10.12989/scs.2021.40.4.495

[17] Sinha, A. K.; Singh, S. Structural response control of RCC moment resisting frame using fluid viscous dampers. *International Journal of Civil Engineering and Technology (IJCIET)*, 2017, 8 (1), pp. 900-910.

[18] Sinha, A. K.; Singh, S. Seismic protection of RC frames using friction dampers. *International Journal of Civil Engineering and Technology (IJCIET)*, 2017, 8 (2), pp. 289-299.

[19] Javidan, Mohammad Mahdi, and Jinkoo Kim. Steel hysteretic column dampers for seismic retrofit of soft-first-story structures. *Steel and Composite Structures*, 2020, 37 (3), pp. 259-272. https://doi.org/10.12989/scs.2020.37.3.259

[20] Dilsiz, A.; Mohammes, M. S.; Moustafa, M. A.; Özuygur, A. R. Seismic design and performance of reinforced concrete special moment resisting frames with wall dampers. *Journal of Earthquake Engineering*, 2022, 26 (2), pp. 744-763. https://doi.org/10.1080/13632469.2019.1692741

[21] Hur, M.-W.; Lee, Y.; Jeon, M.-J.; Lee, S.-H. Seismic Strengthening of RC Structures Using Wall-Type Kagome Damping System. *Buildings*, 2022, 12 (1). https://doi.org/10.3390/buildings12010041

[22] Wang, G. et al. Modeling and experimental investigation of a novel arc-surfaced frictional damper. *Journal of Sound and Vibration*, 2017, 389, pp. 89-100. https://doi.org/10.1016/j.jsv.2016.11.019

[23] Bagheri, S.; Barghian, M.; Saieri, F.; Farzinfar, A. U-shaped metallic-yielding damper in building structures: Seismic behavior and comparison with a friction damper. *Structures*, 2015, 3, pp. 163-171. https://doi.org/10.1016/j.istruc.2015.04.003

[24] Aghlara, R.; Tahir, M. Md. A passive metallic damper with replaceable steel bar components for earthquake protection of structures. *Engineering Structures*, 2018, 159, pp.185-197. https://doi.org/10.1016/j.engstruct.2017.12.049

[25] Wu, C. et al. Experimental study on precast concrete moment-resisting frame system with sector lead viscoelastic dampers. *Structural Control and Health Monitoring*, 2021, 28 (7). https://doi.org/10.1002/stc.2746

[26] Zhang, C.; Huang, W.; Zhou, Y.; Luo, W. Experimental and numerical investigation on seismic performance of retrofitted RC frame with sector lead viscoelastic damper. *Journal of Building Engineering*, 2021, 44. https://doi.org/10.1016/j.jobe.2021.103218

[27] Bruschi, E.; Zoccolini, L.; Cattaneo, S.; Quaglini, V. Experimental Characterization, Modeling, and Numerical Evaluation of a Novel Friction Damper for the Seismic Upgrade of Existing Buildings. *Materials*, 2023, 16 (5). https://doi.org/10.3390/ma16051933

[28] Fathizadeh, S. F. et al. Trade-off Pareto optimum design of an innovative curved damper truss moment frame considering structural and non-structural objectives. *Structures*, 2020, 28, pp. 1338-1353. https://doi.org/10.1016/j.istruc.2020.09.060

[29] Fathizadeh, S. F. et al. Seismic performance assessment of multi-story steel frames with curved dampers and semi-rigid connections. *Journal of Constructional Steel Research*, 2021, 182. https://doi.org/10.1016/j.jcsr.2021.106666

[30] Aydin, E. et al. Improvement of building resilience by viscous dampers. In: *Resilient Structures and Infrastructure*, Farsangi, E. N. et al. (eds.). Singapore: Springer Singapore; 2019, pp. 105-127. https://doi.org/10.1007/978-981-13-7446-3_4

[31] Khalili, M.; Sivandi-Pour, A.; Farsangi, E. N. Experimental and numerical investigations of a new hysteretic damper for seismic resilient steel moment connections. *Journal of Building Engineering*, 2021, 43. https://doi.org/10.1016/j.jobe.2021.102811

[32] Brandonisio, G. et al. Seismic design of concentric braced frames. *Journal of Constructional Steel Research*, 2012, 78, pp. 22-37. https://doi.org/10.1016/j.jcsr.2012.06.003

[33] Grande, E.; Rasulo, A. Seismic assessment of concentric X-braced steel frames. *Engineering Structures*, 2013, 49, pp. 983-995. https://doi.org/10.1016/j.engstruct.2013.01.002

[34] Hajirasouliha, I.; Doostan, A. A simplified model for seismic response prediction of concentrically braced frames. *Advances in Engineering Software*, 2010, 41 (3), pp. 497-505. https://doi.org/10.1016/j.advengsoft.2009.10.008

[35] Jazany, R. A.; Hajirasouliha, I.; Farshchi, H. Influence of masonry infill on the seismic performance of concentrically braced frames. *Journal of Constructional Steel Research*, 2013, 88, pp. 150-163. https://doi.org/10.1016/j.jcsr.2013.05.009

[36] Lumpkin, E. J. et al. Investigation of the seismic response of three-story special concentrically braced frames. *Journal of Constructional Steel Research*, 2012, 77, pp. 131-144. https://doi.org/10.1016/j.jcsr.2012.04.003

[37] Koutsoloukas, L.; Nikitas, N.; Aristidou, P. Passive, semi-active, active and hybrid mass dampers: A literature review with associated applications on building-like structures. *Developments in the Built Environment*, 2022, 12. https://doi.org/10.1016/j.dibe.2022.100094

[38] Joseph, J. S. *Link Beam Column System for Seismic Resistance of Reinforced Concrete Structures*. [doctoral thesis], Karunya University, Department of Civil Engineering, Coimbatore, India, 2018. Accessed: 24 October 2023. Available at: https://shodhganga.inflibnet.ac.in/handle/10603/251790

[39] Yu, Z. et al. Seismic performance of precast concrete columns with Improved U-type reinforcement ferrule connections. *International Journal of Concrete Structures and Materials*, 2019, 13 (54). https://doi.org/10.1186/s40069-019-0368-6

[40] Garevski, M., Hristovski, V.; Talaganov, K.; Stojmanovska, M. Experimental investigations of 1/3-scale RC frame with infill walls building structures. In: *13th World Conference on Earthquake Engineering: conference proceedings*. 1-6 August 2004, Vancouver, British Columbia, Canada, 13 WCEE Secretariat; 2004.

[41] Bureau of Indian Standards. Indian Standard IS 10262:2009 – Concrete mix proportioning - Guidelines. Accessed: 24 October 2023. Available at: https://law.resource.org/pub/in/bis/S03/is.10262.2009.pdf

[42] Bureau of Indian Standards. Indian Standard IS 1786:2008 - High strength deformed steel bars and wires for concrete reinforcement – specification. Accessed: 24 October 2023. Available at: https://www.spongeiron.in/standards/is.1786.2008.pdf